The Plant Cell, Vol. 26: 1256–1266, March 2014, www.plantcell.org

Kinesins Have a Dual Function in Organizing Microtubules during Both Tip Growth and Cytokinesis in *Physcomitrella patens*[W][OPEN]

Yuji Hiwatashi,[a,1] Yoshikatsu Sato,[b] and John H. Doonan[a]

[a] National Plant Phenomics Centre, Institute of Biological, Environmental, and Rural Sciences (IBERS), Aberystwyth University, Gogerddan, Aberystwyth SY23 3EB, United Kingdom

[b] Institute of Transformative Bio-Molecules (WPI-ITbM), Nagoya University, Furo-cho, Chikusa-ku, Nagoya 464-8602, Japan

ORCID IDs: 0000-0002-3996-0549 (Y.H.); 0000-0001-6027-1919 (J.H.D.)

Microtubules (MTs) play a crucial role in the anisotropic deposition of cell wall material, thereby affecting the direction of growth. A wide range of tip-growing cells display highly polarized cell growth, and MTs have been implicated in regulating directionality and expansion. However, the molecular machinery underlying MT dynamics in tip-growing plant cells remains unclear. Here, we show that highly dynamic MT bundles form cyclically in the polarized expansion zone of the moss *Physcomitrella patens* caulonemal cells through the coalescence of growing MT plus ends. Furthermore, the plant-specific kinesins (KINID1) that are is essential for the proper MT organization at cytokinesis also regulate the turnover of the tip MT bundles as well as the directionality and rate of cell growth. The plus ends of MTs grow toward the expansion zone, and KINID1 is necessary for the stability of a single coherent focus of MTs in the center of the zone, whose formation coincides with the accumulation of KINID1. We propose that KINID-dependent MT bundling is essential for the correct directionality of growth as well as for promoting growth per se. Our findings indicate that two localized cell wall deposition processes, tip growth and cytokinesis, previously believed to be functionally and evolutionarily distinct, share common and plant-specific MT regulatory components.

INTRODUCTION

A wide range of tip-growing cells in fungi, animals, and plants display polarized cell growth, which is an essential cellular process for the form and function of the individual cell. Vesicles containing new cell wall components and membranes are secreted continuously and specifically into the apical dome, and coupled with turgor pressure–driven cell expansion, this restricts growth to this limited zone. Understanding the regulatory mechanisms underlying tip growth in land plants has been advanced through the use of three main cell types: moss protonemata and root hairs and pollen tubes of seed plants. The relationship between the cytoskeleton, anisotropic deposition of the cell wall, and polar exocytosis has been a subject of much interest (Rounds and Bezanilla, 2013).

Microtubules (MTs) are fundamental components of the plant cytoskeleton and play a number of critical functions during the plant cell cycle, from modeling the cell wall during interphase to the assembly of the preprophase band, spindle, and phragmoplast during cell division (Brown and Lemmon, 2001). In tip-growing cells, MTs reside on the cell cortex in a generally longitudinal orientation and contribute to tip growth. In many angiosperm pollen tubes, disruption of the MTs has no apparent effect on growth (Cai and Cresti, 2010), but it has recently been reported to affect both endocytosis and exocytosis in the tip of tobacco (*Nicotiana tabacum*) pollen tubes (Idilli et al., 2013). The growth of gymnosperm pollen tubes is inhibited by MT-depolymerizing drugs (Anderhag et al., 2000; Justus et al., 2004). In growing root hairs, the loss of MTs leads to wavy growth and bifurcated tips (Bibikova et al., 1999). In moss, protonemata treated with MT-depolymerizing drugs produce bent, swollen, or even multiple tips (Doonan et al., 1988). These results suggest that MTs play a role in defining the site of growth in diverse tip-growing cells, but it remains unclear how MT dynamics are regulated in the growing apical dome.

MT-based motor proteins of the kinesin family accumulate in tip-growing cells, suggesting that kinesins play roles during tip growth (Yang et al., 2007; Cai and Cresti, 2010; Lazzaro et al., 2013). Kinesins are essential for many critical cellular processes, and the way in which kinesins fulfill these diverse functions may be broadly classified into two categories: MT organization and MT-based activities (Shen et al., 2012; Zhu and Dixit, 2012). Kinesins contribute to MT organization through a variety of mechanisms, including the regulation of MT dynamics, cross-linking of MTs into bundles, and translocation of MTs. MT-based kinesin function typically entails the directional transport of cellular components. Most kinesins identified in pollen tubes are hypothesized to be associated with organelle movement, such as Golgi bodies and mitochondria (Cai and Cresti, 2010; Lazzaro et al., 2013). Conversely, a plant-specific kinesin, MRH2, likely functions in MT organization in root hairs (Yang et al., 2007), but little is known about how kinesins regulate the MT dynamics responsible for plant tip growth.

Apical caulonemal cells of the moss *Physcomitrella patens* grow by means of tip growth (Menand et al., 2007) and have a transparent

[1] Address correspondence to yuh6@aber.ac.uk.
The author responsible for distribution of materials integral to the findings presented in this article in accordance with the policy described in the Instructions for Authors (www.plantcell.org) is: Yuji Hiwatashi (yuh6@aber.ac.uk).

[W] Online version contains Web-only data.

[OPEN] Articles can be viewed online without a subscription.

www.plantcell.org/cgi/doi/10.1105/tpc.113.121723

apical zone where very rapid polarized expansion occurs (Vidali and Bezanilla, 2012; Rounds and Bezanilla, 2013); therefore, they are ideal for studies of tip growth. We previously identified plant-specific kinesins (KINID1) indispensable for the formation of antiparallel bundles of the phragmoplast MTs during cell division (Hiwatashi et al., 2008). These kinesins also accumulate in the apical dome, suggesting that they are associated with MT organization during tip growth. In this article, using a combination of live-cell imaging and genome engineering, we demonstrate that KINID1 kinesins are essential for tip growth. The MT plus ends grow toward the apical expansion zone and converge to a single point in the center of the apical dome, resulting in the dynamic formation of intense MT bundles. We show that the formation and disappearance of the intense MT bundles are regulated by KINID1a and KINID1b, indicating that MT plus end bundling by KINID1 occurs in two different cellular processes, tip growth and cytokinesis, that involve the localized deposition of cell wall.

RESULTS

MT Plus Ends Bundle to Form Dynamic Foci That Correlate with Cell Expansion

To investigate MT distribution in living caulonemal apical cells, we used a transgenic *P. patens* line stably expressing the synthetic green fluorescent protein (sGFP)-α-tubulin (Hiwatashi et al., 2008). The GFP-labeled cytoplasmic MTs were aligned longitudinally throughout the cytoplasm of the cells and converged in the tip of the growing apical cell (Supplemental Figure 1), consistent with previous studies using indirect immunofluorescence staining with antitubulin antibodies (Doonan et al., 1988).

To study MT dynamics, we next visualized the growing plus ends of MTs using EB1b, one of three *P. patens* proteins homologous to EB1 that enabled us to track the growing plus ends (Supplemental Figure 2A) (Chan et al., 2003). A yellow fluorescent protein (Citrine) (Griesbeck et al., 2001) was inserted in-frame before the stop codon of *EB1b* in its genomic locus by homologous recombination (Supplemental Figure 2B). This transgenic line (EY47) contains a single insertion and displayed no detectable growth retardation or morphological defects (Supplemental Figures 2C and 2D). EB1b-Citrine–marked plus ends were evenly distributed throughout the cytoplasm of the apical cells (Figure 1A). As shown in kymographs of the EB1b-Citrine comets in the apical region of the cells, the majority of growing plus ends moved to the apical side (Figure 1B; Supplemental Movie 1). Within the apical dome of the growing cells, ~97% of the comets moved toward the apical expansion zone (Figure 1C), indicating that the MTs predominantly polymerize toward the expansion zone.

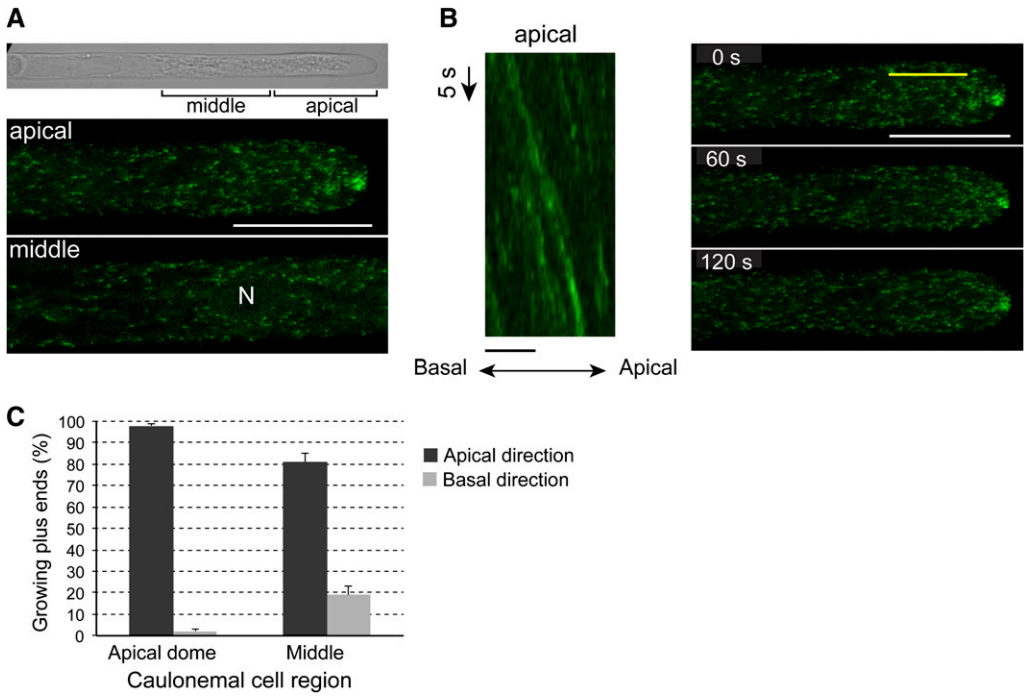

Figure 1. Dynamics of Plus Ends of Growing MTs and Formation of Intense MT Bundles in Growing Apical Domes of Caulonemal Apical Cells.

(A) Distribution of EB1b-Citrine in a caulonemal apical cell. Images were acquired every 1 s. Representative images shown are maximum Z-projections of three planes (0.7-μm intervals), with the apex of the cell always located on the right side of the image. N, nucleus. Bar = 20 μm.

(B) Kymographs of EB1b-Citrine obtained from regions as indicated by the yellow line in the top right panel. Kymographs display a period of 2 min (Supplemental Movie 1). The right and left sides of the panels are oriented to the apical and basal directions, respectively. Black and white bars = 5 μm and 20 μm, respectively.

(C) Direction of growing plus ends in the apical domes. The number of growing MT plus ends was counted in the apical dome (at 8 μm distance from a tip; $n > 100$) and the middle region (at 90 μm distance from a tip; $n > 50$) of apical cells ($n = 3$). Error bars indicate SD ($n = 3$).

Time-lapse microscopy observations showed that MTs converged at a single focus within the center of the apical dome (Figure 2A) in a cyclical manner. The foci developed into an intense MT bundle with the coalescence of additional MTs. During expansion of the tips, the intense MT bundles were formed and then disappeared (arrow in Figure 2B). After their disappearance, new MT bundles were quickly formed (Figure 2B; Supplemental Movie 2). This formation and collapse of the intense MT bundles was repeated continuously in the growing apical dome, suggesting that generation of the intense MT bundles oscillates in a highly dynamic manner.

The EB1b-Citrine comets also converged to a single point in the center of the growing apical dome (Figure 2C), indicating that the growing plus ends were merged with each other. To investigate whether MT bundle formation coincided with the merger of the growing plus ends, we integrated a construct that

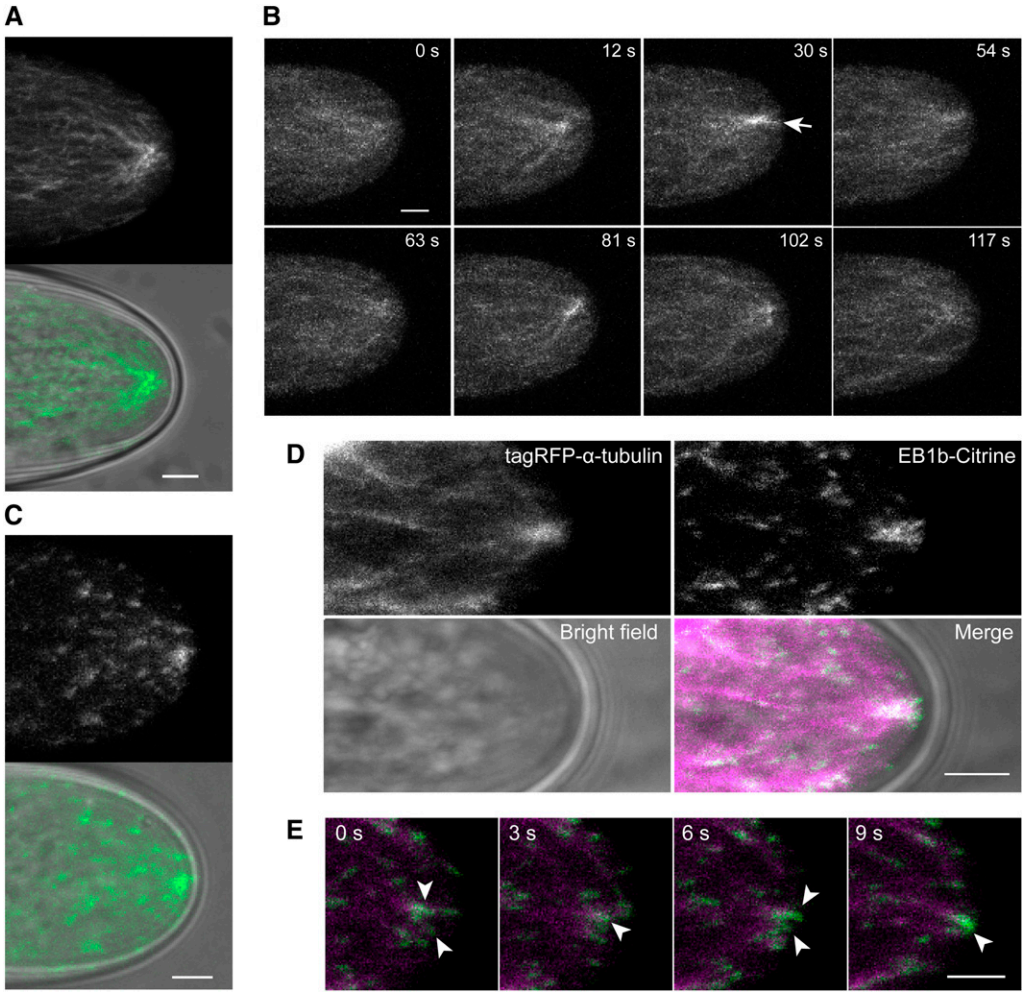

Figure 2. Formation of Intense MT Bundles via the Merger of the Growing Plus Ends of the MTs in Growing Apical Domes.

(A) Distribution of sGFP-α-tubulin in the dome of a caulonemal apical cell. The images are maximum Z-projections of four planes (0.8-μm intervals). The top and bottom panels show an sGFP fluorescence image and a merged image of bright field (gray) and sGFP fluorescence (green), respectively.
(B) Dynamics of sGFP-α-tubulin in the apical dome of a caulonemal apical cell. The images were acquired every 3 min (Supplemental Movie 2), and representative images shown are maximum Z-projections of 10 planes (0.8-μm intervals). The arrow indicates an intense MT bundle.
(C) Distribution of EB1b-Citrine in the apical dome of a caulonemal apical cell. The images are maximum Z-projections of four planes (0.8-μm intervals). The top and bottom panels show a Citrine fluorescence image and a merged image of bright field (gray) and Citrine fluorescence (green), respectively.
(D) Distribution of TagRFP-α-tubulin and EB1b-Citrine in the apical dome of a caulonemal apical cell. The images are maximum Z-projections of three planes (0.8-μm intervals). The top left and right panels show TagRFP-α-tubulin and EB1b-Citrine fluorescence images, respectively. The bottom left and right panels show bight-field and merged images, respectively, of bright field (gray), TagRFP fluorescence (red), and sGFP fluorescence (green).
(E) Dynamics of TagRFP-α-tubulin and EB1b-Citrine in the apical dome of a caulonemal apical cell. The images are maximum Z-projections of four planes (0.8-μm intervals). The images were acquired every 3 min (Supplemental Movie 3). The TagRFP (red) and Citrine (green) fluorescence images are merged. Arrowheads indicate the growing plus ends of MTs converged with other growing plus ends in the apical dome.
Bars = 2 μm.

constitutively expresses α-tubulin fused with a red fluorescent protein (TagRFP) (Merzlyak et al., 2007) into the EY47 line to generate transgenic lines expressing both EB1b-Citirne and TagRFP-α-tubulin (Supplemental Figures 3A and 3B). The resultant lines had no detectable growth retardation or morphological defects (Supplemental Figure 3C). The intense MT bundles colocalized spatially and temporally with the foci of the growing plus ends of MTs in the apical dome (Figure 2D). Time-lapse observation revealed that the growing plus ends of MTs converged with each other at one point in the apical dome (Figure 2E; Supplemental Movie 3). These results indicate that the growing plus ends of MTs merged to a single point, mirroring the behavior of the MT bundles.

The Plant-Specific Kinesins, KINID1, Colocalize to Growing MT Plus Ends and Accumulate in the MT Bundle

In the polarized growth of fungal filamentous cells, such as *Aspergillus nidulans*, growing MTs merge at the center of growing tips to make MT foci (Konzack et al., 2005), and it has been speculated that the resultant MT foci are important for regulating the directionality of growth (Konzack et al., 2005; Steinberg, 2007b; Fischer et al., 2008). In the polarized growth zone of root hair cells of the legume *Medicago truncatula*, MT foci were also detected, but the role of these foci was not reported (Timmers et al., 2007). Therefore, we examined the mechanisms underlying the formation of the intense MT bundles and their involvement in the polarized growth of apical cells.

To gain insight into the formation of the MT bundles, we focused on two plant-specific KINID1 kinesins, KINID1a and KINID1b, because these kinesins were predominantly localized to the tips of caulonemal apical cells and we had previously proposed that they could cross-link the plus ends of phragmoplast MTs, which are a key component of this plant-specific cytokinetic apparatus during cell division (Hiwatashi et al., 2008). Live imaging of growing apical cells expressing both KINID1a-sGFP and mRFP-α-tubulin (Hiwatashi et al., 2008) revealed that KINID1a-sGFP was predominantly colocalized to the intense MT bundles in the growing apical dome (Figure 3A). Similarly, observation of a line expressing both KINID1b-Citrine and mRFP-α-tubulin (Hiwatashi et al., 2008) indicated the KINID1b-Citrine also accumulated in the MT bundles (Figure 3A). Using time-lapse observation, we found that MTs labeled with KINID1a-sGFP were incorporated into the MT foci in the apical dome (Figure 3B; Supplemental Movie 4). These results suggest that the kinesins could be involved in the turnover of the MT bundles in the apical dome.

To obtain a more precise localization of KINID1a and KINID1b relative to the growing MT plus ends, a cyan fluorescent protein (Ceruelan) (Rizzo et al., 2004) gene was inserted into the *KINID1a* or *KINID1b* locus in the background of the line expressing EB1b-Citrine (Supplemental Figure 4). Live-cell imaging revealed that KINID1a-Cerulean and KINID1b-Cerulean were partially localized to the Pp EB1b comets in the apical dome of the growing tips (Figure 4A). We also observed that the KINID1a-Cerulean and KINID1b-Cerulean signals both accumulated in the merged foci of the EB1 comets in the apical dome. Furthermore, we found that the EB1b comets, which are labeled with KINID1a-

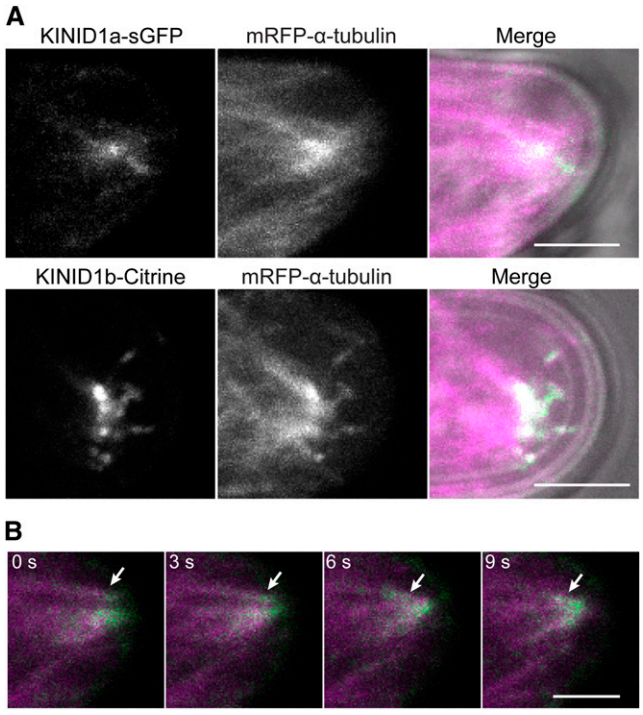

Figure 3. Plant-Specific Kinesins KINID1a and KINID1b Are Predominantly Colocalized to the MT Bundles in Growing Apical Domes of Caulonemal Apical Cells.

(A) Colocalization of KINID1a-sGFP and KINID1b-Citrine with TagRFP-α-tubulin in the apical dome. The sGFP or Citrine fluorescence (green), TagRFP fluorescence (magenta), and bright field (gray) are merged in the right panels. The images are maximum Z-projections of four planes (0.8-μm intervals). Bars = 2 μm.

(B) Dynamics of KINID1a-sGFP and TagRFP-α-tubulin in the apical dome. The sGFP fluorescence (green) and TagRFP fluorescence (magenta) are merged. The images are maximum Z-projections of four planes (0.8-μm intervals). The images were acquired every 3 min (Supplemental Movie 4). Arrows indicate the MTs incorporated into the MT bundle in the apical dome. Bar = 2 μm.

Cerulean and KINID1b-Cerulean, were incorporated into the MT bundles (Figure 4B; Supplemental Movie 5). These results indicate that KINID1a and KINID1b are localized to the growing plus ends of MTs that converged to the MT bundles. Moreover, the accumulation of both KINID1a-Cerulean and KINID1b-Cerulean was also observed in the region basal to the intense EB1 comet foci in the apical dome (Figure 4A). Together with colocalization of these kinesins to MT bundles (Figure 3A), KINID1a and KINID1b are also associated with the MT bundles where growing plus ends of MTs do not accumulate.

Double Deletion of *KINID1a* and *KINID1b* Leads Aberrant Formation and Maintenance of the Intense MT Foci in the Apical Dome

To clarify the roles of KINID1 in the turnover of the intense MT bundles in the center of the growing apical dome, double deleted mutants for the redundant *KINID1a* and *KINID1b* were

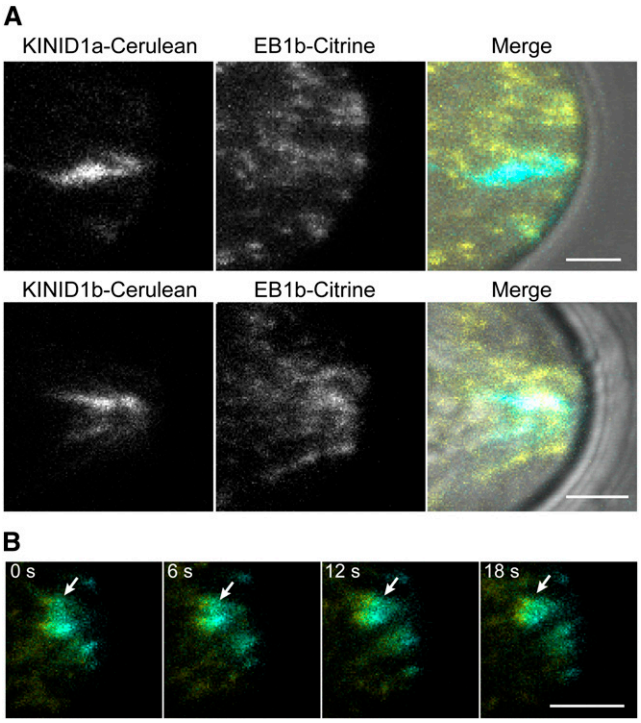

Figure 4. Plant-Specific Kinesins KINID1a and KINID1b Are Predominantly Colocalized to the Growing Plus Ends, Which Are Converged in the Foci of Growing Plus Ends.

(A) Colocalization of KINID1a-Cerulean and KINID1b-Cerulean with EB1b-Citrine in an apical dome. The images are maximum Z-projections of four planes (0.7-μm intervals). The Cerulean fluorescence (cyan), Citrine fluorescence (yellow), and bright field (gray) are merged in the right panels. Bars = 2 μm.

(B) Dynamics of KINID1a-Cerulean and EB1b-Citrine in an apical dome. The Cerulean fluorescence (cyan) and Citrine fluorescence (yellow) are merged. The images are maximum Z-projections of four planes (0.7-μm intervals). The images were acquired every 3 min (Supplemental Movie 5), and representative images are shown. Arrows indicate the growing plus ends merged into one point. Bar = 2 μm.

selected and MT dynamics were observed using sGFP-α-tubulin (Hiwatashi et al., 2008). MT bundles were detected within the apical dome of the double deletion mutants, but their dynamics and stability were severely perturbed (Figure 5A; Supplemental Movie 6). The duration of the intense MT bundles in the double deletion mutants (39 and 36 s in Δkinid1a Δkinid1bGTU-82 [*n* = 39] and -126 [*n* = 27], respectively, as median values) was ~2.5-fold shorter than that of the control line (99 s in GTU193 [*n* = 29] as median value) (Figure 5B). Additionally, after the intense MT bundles within the apical dome collapsed, the regeneration of new MT bundles took significantly more time in comparison with regeneration in the control line (Figures 5A and 5B). The interval between disappearance and regeneration in the double deletion mutants (57 and 54 s in Δkinid1a Δkinid1bGTU-82 [*n* = 19] and -126 [*n* = 19], respectively, as median values) was 4.5-fold longer than that in the control line (12 s [*n* = 29] as median value) (Figure 5C). These results indicate that MT bundles do form in the absence of both KINID1a and KINID1b but that there is a significant reduction in the rate of bundle formation and their persistence.

We also found that the position of the intense apical MT bundles was altered in the double deletion mutants (Figure 5D). In the growing tips of the control line, the MT bundles were centrally positioned in the apical dome, but in the double deletion mutants, the apical MT bundles were positioned more randomly. Moreover, multiple or fragmented MT bundles were observed in the apical dome of the double deletion mutants (Figure 5E; 3 of 26 cells and 2 of 22 cells in Δkinid1a Δkinid1bGTU-82 and -126, respectively), whereas the control line did not exhibit multiple MT bundles in the apical dome (*n* = 41 cells).

Double Deletion of *KINID1a* and *KINID1b* Leads to Loss of the Directionality of Growth and Reduced Expansion Rate

We examined the effects of double deletion of *KINID1a* and *KINID1b* on the tip growth of the apical cells. In the double deletion mutant, the morphology of apical cells was changed. While the cells of the control line grew relatively straight, the double deletion mutants produced curly or curved apical cells (Figure 6A). The proportion of the apical cells with curved tips in the double deletion mutants (56.5% and 61.1% in Δkinid1a Δkinid1bGTU-82 [*n* = 23] and -126 [*n* = 19], respectively) was 8-fold higher than that in the control line (7.1% [*n* = 28]) (Figure 6B). These results indicate that *KINID1a* and *KINID1b* double deletion leads to loss of control over the directionality of growth.

A previous study indicated that the colony diameter of the *KINID1a* and *KINID1b* double deletion mutants was smaller that that in the control line, suggesting that their double deletion also affects the expansion rate of growth (Hiwatashi et al., 2008). Thus, we measured the expansion rate of the tip of the double deletion mutant. The double deletion mutants showed a 25% reduction in the expansion rate (Δkinid1a Δkinid1bGTU-82 [*n* = 23] and -126 [*n* = 19]) in comparison with the control line (*n* = 26), indicating that these kinesins are also required for optimal growth rate (Figure 6C).

DISCUSSION

KINID1 at MT Plus Ends Is Necessary for the Formation and Stability of a Single MT Bundle at the Center of the Expanding Zone

Our time-lapse observation with EB1-Citrine revealed that the growing plus ends of MTs are oriented to the apical dome. This result is consistent with previous studies in other tip-growing cells such as the legume *M. truncatula* (Timmers et al., 2007) and the filamentous fungi *Ustilago maydis* (Schuchardt et al., 2005) and *A. nidulans* (Konzack et al., 2005), indicating that the plus ends of MTs are orientated toward the actively growing tips. This supports the idea that the polarity of MT growth during polarized tip growth is evolutionarily conserved across a wide phylogeny.

Our results demonstrate that the plant-specific kinesins, KINID1, colocalize strongly to growing plus ends of MTs, which

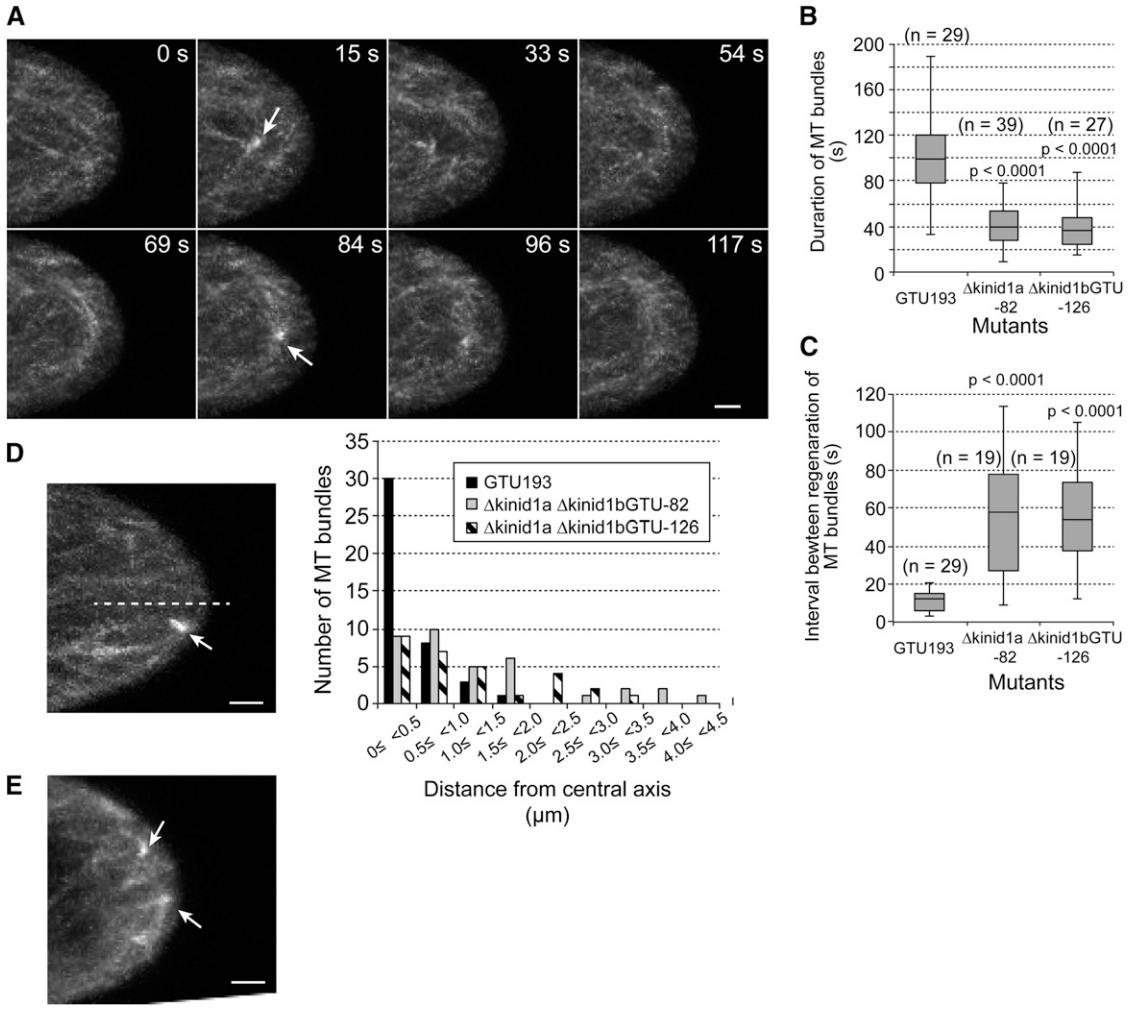

Figure 5. Plant-Specific Kinesins KINID1a and KINID1b Are Required for Correct Formation and Maintenance of the Intense MT Bundles in Apical Domes of Caulonemal Apical Cells.

(A) Dynamics of sGFP-α-tubulin in an apical dome of a caulonemal apical cell of *KINID1a* and *KINID1b* deletion mutants. The images were acquired every 3 min (Supplemental Movie 6), and representative images are shown. The images are maximum Z-projections of 10 planes (0.8-μm intervals). Arrows indicate the MT bundles. Bar = 2 μm.

(B) Measurement of the appearance duration of the intense MT bundle in apical domes of caulonemal apical cells of the control line (GTU193) and the *KINID1a* and *KINID1b* double deletion mutants (Δkind1a Δkinid1bGTU-82 and -126). The graph shows box-plot medians and 25th/75th percentiles. $P < 0.0001$, unpaired *t* test between the control line and the mutants.

(C) Measurement of the interval duration between generation of the intense MT bundles in apical domes of caulonemal apical cells of the control line (GTU193) and the *KINID1a* and *KINID1b* double deletion mutants (Δkind1a Δkinid1bGTU-82 and -126). The graph shows box-plot medians and 25th/75th percentiles. $P < 0.0001$, unpaired *t* test between the control line and the mutants.

(D) Distribution of intense MT bundles in apical domes. The left image shows an MT bundle (arrow) positioned from a central axis (dotted line) in an apical dome of the *KINID1a* and *KINID1b* double deletion mutant (Δkinid1a Δkini1bGTU-82). The graph at right indicates the number of MT bundles relative to the distance from a central axis on the apical dome. Bar = 2 μm.

(E) Multiple MT bundles in an apical dome of the *KINID1a* and *KINID1b* double deletion mutant. Arrows indicate the MT bundles. Bar = 2 μm.

are incorporated into the intense MT bundles, and accumulate in the MT bundle in the apical dome. Therefore, we reasoned that KINID1a and KINID1b on the MT plus ends might function in the merger of the growing plus ends into the MT bundles, although we cannot exclude the possibility that these kinesins are already present at the MT plus end–converging point. The idea that KINID1 is required for bundle formation or dynamics is supported by the observation that the formation of the intense MT bundle is significantly reduced in *KINID1* double deletion mutants. Furthermore, double deletion of *KINID1* led to the early collapse of the MT bundles, clearly indicating that these kinesins are required for normal maintenance of the intense MT bundles

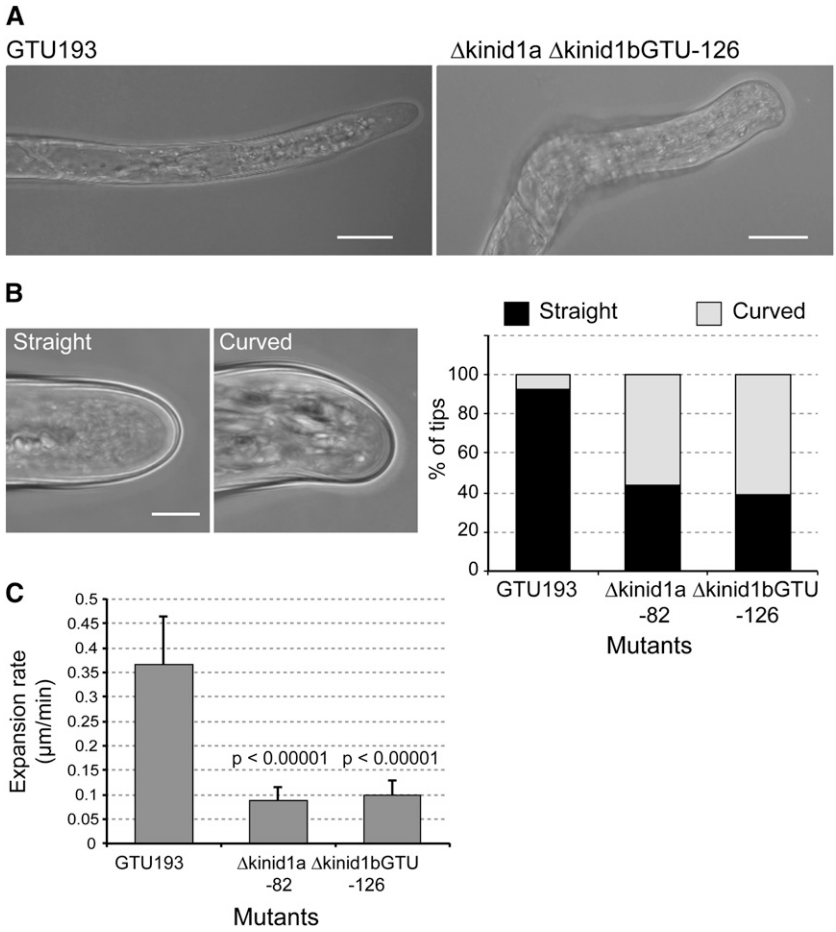

Figure 6. Double Deletion of *KINID1a* and *KINID1b* Leads to Both Misdirection and Reduced Expansion Rate of Tip Growth.

(A) Shape of caulonemal apical cells in the control line and in the *KINID1a* and *KINID1b* double deletion mutant. Bars = 20 μm.

(B) Proportion of tips showing straight and curved shapes. The straight and curved sets of tip shape are designated. Bar = 5 μm.

(C) Expansion rate of tip growth for caulonemal apical cells of the control line and the *KINID1a* and *KINID1b* double deletion mutants. The expansion rate was measured by time-lapse imaging (interval of 3 s, duration of 340 s) of the GTU193 line (n = 28) and the double deletion mutants Δkinid1a Δkinid1bGTU-82 (n = 18) and Δkinid1a Δkinid1GTU-126 (n = 22). $P < 0.0001$, unpaired t test between the control line and the mutants. Error bars indicate SD.

in the apical dome. Together with the localization pattern of these kinesins, we propose that the KINID1 kinesins are essential for the efficient merger of plus ends of MTs into a single point and also for the maintenance of the resulting MT bundles in the center of the apical dome (Figure 7). An EB1 binding motif, Ser-x-Ile-Pro (SxIP), acts as an MT tip localization signal, suggesting that MT plus end–tracking proteins with the motif are targeted to growing plus ends by binding to EBs (Honnappa et al., 2009). The SxIP motif was found in the amino acid sequences of both KINID1a and KINID1b (residues 322 to 325 and 319 to 322 in KINID1a and KINID1b, respectively), and its presence suggests that the kinesins could be recruited to the growing plus ends in the apical dome via the SxIP motif in an EB1-dependent manner.

Kinesins identified in plant tip-growing cells have been reported in a variety of species (Yang et al., 2007; Cai and Cresti, 2010; Lazzaro et al., 2013), and it is very likely that most of these kinesins support tip growth by delivering a diverse spectrum of cargo along MTs to an expansion zone. A mutation in another plant-specific kinesin gene, *MRH2*, leads to fragmentation and random orientation of MTs in root hairs in *Arabidopsis thaliana* (Yang et al., 2007). An ARM domain of MRH2, which is not found in KINID1, might interact with an unknown MT regulator or an unknown cargo binding protein involved in vesicle/organelle transport. Our study suggests that the KINID1 are involved in the formation and maintenance of the MT bundle by merging the growing plus ends in the apical dome. Thus, the possible roles of KINID1 are likely different from that of MRH2, which suggests a novel role of a kinesin in MT organization during plant polarized growth.

It is interesting that the role of KINID1 in MT organization during tip growth is reminiscent of the function of KipA

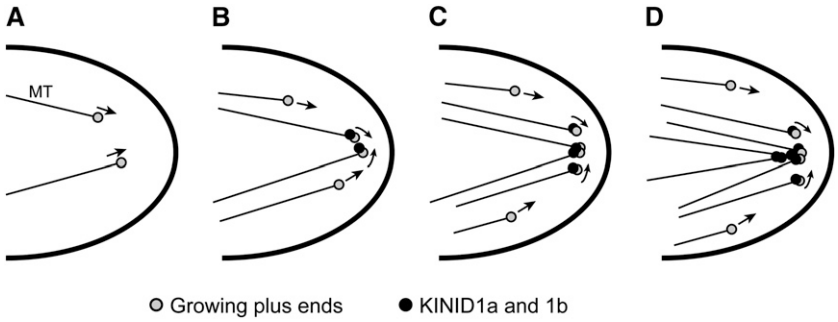

Figure 7. Schematic Representation of the Formation of Intense MT Bundles in an Apical Dome Proposed in This Study.

(A) MTs polymerize to an apical dome. Arrows represent the direction of MT growth.
(B) KINID1-labeled growing plus ends approach each other in the center of the apical dome.
(C) KINID1-labeled growing plus ends merge at a single point (focus) underneath the cell periphery.
(D) MT bundles labeled with KINID1 are formed. The growing activity of the plus ends is possibly suppressed. KINID1 could regulate the formation and maintenance of the MT bundles.

(a member of the kinesin-7 family) in hypha growth of the filamentous fungus *A. nidulans* (Konzack et al., 2005). KipA localizes at plus ends of MTs and is thought to focus and anchor the MT plus ends to the growing hyphal apex. However, such a role for kinesin-7 was not found in the basidiomycete *U. maydis* (Schuchardt et al., 2005), raising doubts about a general role of these kinesins in tip growth. Interestingly, *Arabidopsis* PAKRP (orthologous to the KINID1 kinesins) was proposed to contribute to vesicle transfer in the phragmoplast (Lee et al., 2001), which is different from the roles of KINID1 proposed in this study. Consistent with distinct roles, the defects of phragmoplast MTs observed in the *KINID1* double deletion mutants were not restored by the ectopic expression of PAKRP (Hiwatashi et al., 2008). Therefore, it seems likely that the function of KINID1 and KipA in MT organization may have evolved in a lineage-specific manner.

Plant-Specific Kinesins Promote Tip Growth and Regulate the Direction of Growth

Disruption of MT organization indicates that organization per se could be essential for plant tip-growing cells (Rounds and Bezanilla, 2013) as well as fungal hyphae (Steinberg, 2007a). Therefore, it seems likely that MT disorganization in the apical dome is responsible for the defects of polarized growth detected in the *KINID1* double deleted cell, although it cannot be excluded that the KINID1 kinesins are involved in determining directionality and promoting expansion independently of their effects on MT organization. In *A. nidulans*, KitA anchors MTs at the center of a growing tip and seems to be indispensable for positioning the Spitzenkörper (the vesicle supply center), which plays a major role in determining growth directionality (Konzack et al., 2005). The intense MT bundles are positioned in the center of the local expansion zone by a mechanism that requires the KINID1 kinesins, and the anisotropic deposition of cell wall and polar exocytosis associated with the intense MT bundles could be involved in determining the growth directionality. This hypothesis is strongly supported by pharmacological analysis with an MT-depolymerizing drug, oryzalin. A low-dose application of the MT-depolymerizing drug on caulonemal cells led to a reduction in the duration of bundles, multiple bundle formation, and bundle mispositioning in the apical dome (Supplemental Figure 5). Moreover, the cells treated with the drug showed loss of growth directionality and reduction of expansion (Supplemental Figure 6). These defects caused by drug application mimic the defects in MT dynamics and tip growth observed in the *KINID1* double deletion mutants.

An alternative explanation is that KINID1 could transport cellular components, such as cell wall precursors, to the center of the apical dome and that cell growth defects in the double mutant could be due to the perturbation of such a function. In *U. maydis* hyphae, kinesin-3 moves as dots and accumulates near the tip, suggesting that kinesin-3 delivers its cargo (including secretory vesicles) to the polar growth region along MTs (Schuchardt et al., 2005). However, we could not detect a dot-like movement of KINID1, suggesting that it is not primarily associated with cargo transport. The investigation of vesicle dynamics in the growing apical dome will offer insight into this possibility.

It is generally accepted that the actin cytoskeleton is essential for tip growth in all cell types, including protonemata, root hairs, and pollen tubes (Rounds and Bezanilla, 2013), as well as hypha (Steinberg, 2007a). Previous studies on F-actin organization and actin-associated proteins reveal that the actin cytoskeleton is essential for polarized cell growth in moss cells (Doonan et al., 1988; Vidali and Bezanilla, 2012). In apical cells expressing Lifeact-mEGFP, an actin focal point is also observed in the apical dome (Vidali et al., 2009). The microtubule-associated protein MAP18 functions in the direction of pollen tube growth by modulating actin filaments in *Arabidopsis* (Zhu et al., 2013). MAP18 can bind the MTs in vivo and is associated with cortical MTs in epidermis cells (Wang et al., 2007). Proteins interacting with both MTs and F-actin have been reported in plants (Petrásek and Schwarzerová, 2009), and it is possible that the MT bundles regulated by KINID1 could also interact with the F-actin organization, although it remains unclear whether the intense MT bundles correspond to the actin focal point.

Plant-Specific Kinesins Have a Shared Function in Tip Growth and Cytokinesis through the Bundling of MTs at the Plus End

During phragmoplast development, the plus ends of MTs are interdigitated at the phragmoplast equator (Hepler and Jackson, 1968; Hiwatashi et al., 2008; Ho et al., 2011). In tobacco BY-2 cells, MT bundles are also formed at the leading edge of the phragmoplast, through the bundling of plus ends of antiparallel MTs (Murata et al., 2013). Our findings suggest that the formation of the intense MT bundles in the growing apical dome is functionally similar to the bundling of the plus ends of MTs in the phragmoplast, in terms of the merging of the plus ends of the MTs, although the intense MT bundles are likely formed with parallel MTs. Both processes may be regulated by shared regulatory mechanisms, as the KINID1 kinesins are indispensable also for the interdigitating plus ends of the phragmoplast MTs at cytokinesis (Hiwatashi et al., 2008). Their role in merging the plus ends of cytoplasmic MTs, as proposed here, is likely to be consistent with that in cross-linking the plus ends of phragmoplast MTs to generate the MT bundles at cytokinesis. Therefore, we speculate that the KINID1 kinesins have a shared function in the MT organization of two different cellular processes, tip growth and cytokinesis, that were previously thought to be quite distinct. The mechanism for dual targeting of kinesins to these different cellular processes is still an open question, and the targeting mechanism will help explain how molecular machineries responsible for managing MT organization have been recruited during the evolution of divergent cellular processes.

METHODS

Moss Materials and Transformation

Physcomitrella patens subsp *patens* collected in Gransden Woods (Ashton and Cove, 1977) was used as the wild-type line. The moss lines were cultured on BCDAT medium under continuous white light at 25°C (Nishiyama et al., 2000). Transformation was performed by the polyethylene glycol–mediated method as described previously (Nishiyama et al., 2000).

Construction of Plasmids for Gene Targeting

Primer sequences are listed in Supplemental Table 1. All lines obtained by gene targeting were verified by genomic DNA gel blot analysis.

To construct EB1b-Citrine lines, an *EB1b* genomic DNA fragment spanning the middle to the last codon of the coding region was PCR amplified with the PpEB1bF1 and PpEB1bR1 primers using *P. patens* genomic DNA as a template, digested with *Sal*I, and cloned in the *Sal*I and *Eco*RV sites of the pCTRN-NPTII2 plasmid, thereby creating an in-frame fusion of the *EB1* coding sequence and the modified yellow fluorescent protein gene *Citrine* (Griesbeck et al., 2001). A genomic DNA fragment downstream of the stop codon of *EB1b* was PCR amplified with the PpEB1bF2 and PpEB1bR2 primers, digested with *Not*I and *Sac*II, and cloned into the *Not*I and *Sac*II sites of the plasmid to make the pEB1b-Citrine plasmid. The pEB1b-Citrine plasmid was digested with *Sal*I and *Sac*II for gene targeting.

To express the TagRFP-α-tubulin fusion protein in the moss, the pKH1-TagRFP-α-tubulin plasmid was constructed as below. A DNA fragment covering the promoter region of *KINID1a* (Kubo et al., 2013) was PCR amplified with the API1pF1 and API1pR1 primers using *P. patens* genomic DNA as a template, digested with *Kpn*I, and cloned into the *Kpn*I and *Eco*RV sites of pTN90 (Hiwatashi et al., 2008) to produce pKH1. A *TagRFP* (Merzlyak et al., 2007) gene fragment was PCR amplified with tagRFPstart and tagRFPend primers using Gateway TagRFP-AS-N plasmid (Evrogen) as a template and cloned in an *Eco*RV site of pBluescript II (Agilent Technologies) to make pBS-TagRFP. A DNA fragment including a coding region of the α-tubulin gene was PCR amplified using the p35S-sGFP-ad2-tubulin plasmid (Hiwatashi et al., 2008) as a template, digested with *Eco*RI, and cloned into the *Eco*RI and *Sma*I sites of pBS-TagRFP, thereby creating in-frame fusion genes encoding tagRFP-α-tubulin. A DNA fragment encoding the TagRFP-α-tubulin fusion protein was PCR amplified with tagRFPstartF2 and PpTUArApaI, digested with *Apa*I, and cloned into the *Apa*I and *Sma*I sites of the pKH1 plasmid to make pKH1-TagRFP-α-tubulin plasmid. The plasmid was digested with *Not*I for gene targeting.

To generate KINID1a-Cerulean and KINID1b-Cerulean lines, a DNA fragment of the aphIV cassette (amplified with aph4F1 and aph4R1 using pTN186 as a template for PCR) was ligated with a DNA fragment containing the modified cyan fluorescent protein gene *Cerulean* (Rizzo et al., 2004), the nopaline synthase polyadenylation signal, and two loxP sites that were PCR amplified with CeruF1 and CeruR1 primers using pCerulean-NPTII plasmid as a template to make pCerulean-aphIV. A DNA fragment containing the coding region of *sGFP* and an NPTII cassette in the pAPI1GFP and pAPI1LCitrine plasmids (Hiwatashi et al., 2008) was replaced with a DNA fragment covering the coding region of Cerulean and the aphIV cassette from the pCerulean-aph4 plasmid with *Sal*I and *Spe*I to produce API1Cerulean and API1LCerulean plasmids, respectively. For gene targeting, the API1Cerulean and API1LCerulean plasmids were digested with *Sac*I and *Not*I-*Apa*I, respectively.

Generation of Gene-Targeting Lines

Primer sequences are listed in Supplemental Table 1. All lines obtained by gene targeting were verified by DNA gel blot analysis. The EY47 line expressing EB1-Citrine was generated by inserting *Citrine* in the *EB1b* locus in the background of the wild type. The EYRT36 lines coexpressing EB1b-Citrine and TagRFP-α-tubulin were obtained by integrating a TagRFP-α-tubulin expression construct into the genome of the EY47 line. The KINID1aCeruleanEY45 line coexpressing KINID1a-Cerulean and EB1b-Citrine was generated by inserting *Cerulean* into the *KINID1a* locus in the background of the EY47 line. The KINID1aCeruleanEY34 and -54 lines coexpressing KINID1b-Cerulean and EB1b-Citrine were generated by inserting *Cerulean* into the *KINID1b* locus in the background of the EY47 line.

DNA Gel Blot Analysis

Procedures for nucleic acid extraction were described previously (Hiwatashi et al., 2001). Genomic DNA was digested with restriction enzymes, run on agarose gels, and transferred to nylon membranes according to previously described procedures (Hiwatashi et al., 2001). Probe labeling was performed using the PCR DIG Probe Synthesis Kit (Roche Diagnostics) according to the supplier's instructions. Hybridization and detection were performed using DIG Easy Hyb (Roche Diagnostics) and CDP-star (Roche Diagnostics) according to the supplier's instructions. A PCR fragment synthesized with PpHB7-3for and PpHB7-3rev primers using the pKH1-tagRFP-α-tubulin plasmid as a template was used as the HB7-3 probe. A PCR fragment amplified with PpEB1bF1 and PpEB1bR1 primers using the pEB1b-Citrine plasmid as a template was used as the EB1b-5 probe.

For KINID1a-Cerulean and KINID1b-Cerulean lines, a PCR fragment amplified with the M13-21 and api1R3940ClaI primers using the pKINID1a-Cerulean plasmid as a template and with the M13-21 and sGFP

primers using the pKINID1b-Cerulean plasmid as a template were used as the KINID1aC and KINID1aC probes, respectively.

Microscopy

For imaging of living cells, protonemal cells were cultured on BCD agar medium supplemented with 1 mM $CaCl_2$ (Nishiyama et al., 2000) in a glass-bottom dish for 7 to 10 d. For application of the MT-depolymerizing drug, protonemata were cultured for 7 to 10 d in the absence and presence of 0.1 and 1 μM oryzalin (Sigma-Aldrich). Image acquisition was performed with an LSM780 inverted confocal laser microscope with a ×63/1.40–numerical aperture objective lens (Carl Zeiss Microscopy).

Time-lapse observations for sGFP-α-tubulin in the GTU193 line and the *KINID1a* and *KINID1b* double deletion mutants were performed using a 488-nm excitation laser and collecting emission spectrum of 490 to 605 nm. Image acquisition was performed at 3-s intervals with Z-scan (0.8-μm intervals, 10 planes).

For time-lapse imaging of EB1b-Citrine, image acquisition was performed at 1-s intervals with Z-scan (0.7-μm intervals, three planes) by using a 488-nm excitation laser and collecting emission spectrum of 490 to 605 nm.

Time-lapse imaging of EB1b-Citrine and TagRFP-α-tubulin was performed at 3-s intervals with Z-scan (0.8-μm intervals, three planes). For Citrine, the 490- to 561-nm emission spectrum was collected using a 488-nm excitation laser. For mRFP, the 570- to 693-nm emission spectrum was collected using a 560-nm excitation laser.

For time-lapse imaging of KINID1a-sGFP and KINID1b-Citrine, together with mRFP-α-tubulin, image acquisition was performed at 3-s intervals with Z-scan (0.8-μm intervals, three planes). A 488-nm excitation laser was used for sGFP and Citrine with collection of emission spectrum from 490 to 561 nm, and a 560-nm excitation laser was used for mRFP by collecting the 570- to 693-nm emission spectrum.

For time-lapse imaging of KINID1a-Cerulenan and KINID1b-Cerulean, together with PpEB1b-Citrine, image acquisition was performed at 3-s intervals with Z-scan (0.8-μm intervals, three planes). Cerulean and Citrine fluorescence were detected using 458- and 514-nm excitation lasers and collecting emission spectra of 464 to 508 nm and 528 to 620 nm, respectively.

Image processing was performed using Fiji (Schindelin et al., 2012) (http://fiji.sc/Fiji).

Accession Numbers

Sequence data from this article can be found in the National Center for Biotechnology Information database under the following accession numbers: *P. patens* genes *KINID1a* (AB434497), *KINID1b* (AB434498) and *EB1b* (XM_001753485); *Arabidopsis* genes *PAKRP2* (At4g14330), *MRH2* (At2g54870), and *MAP18* (At5g44610); and *A. nidulans* gene *KipA* (AJ622826).

Supplemental Data

The following materials are available in the online version of this article.

Supplemental Figure 1. Distribution of sGFP-α-Tubulin in a Caulonemal Apical Cell.

Supplemental Figure 2. Generation of the Lines Expressing EB1b-Citrine.

Supplemental Figure 3. Generation of the Lines Coexpressing EB1b-Citrine and TagRFP-α-Tubulin.

Supplemental Figure 4. Generation of the Lines Coexpressing KINID1a-Cerulean and PpEB1b-Citrine and the Lines Coexpressing KINID1b-Cerulean and EB1b-Citrine.

Supplemental Figure 5. Application of an MT-Depolymerizing Drug, Oryzalin, Leads to Aberrant Formation and Maintenance of the Intense MT Bundles in Apical Domes of Caulonemal Apical Cells.

Supplemental Figure 6. Application of an MT-Depolymerizing Drug, Oryzalin, Leads to Both Misdirection and Reduced Expansion Rate of Tip Growth.

Supplemental Table 1. Primers Used in This Work.

Supplemental Movie 1. Dynamics of EB1b-Citrine Comets in the Apical Region of the Caulonemal Apical Cell.

Supplemental Movie 2. Dynamics of sGFP-α-Tubulin in the Apical Dome of the Control Line.

Supplemental Movie 3. Dynamics of TagRFP-α-Tubulin and EB1b-Citrine in the Apical Dome.

Supplemental Movie 4. Dynamics of KINID1a-sGFP and TagRFP-α-Tubulin in the Apical Dome.

Supplemental Movie 5. Dynamics of KINID1a-Cerulean and EB1b-Citrine in the Apical Dome.

Supplemental Movie 6. Dynamics of sGFP-α-Tubulin in the Apical Dome of the *KINID1* Double Deletion Mutant.

Supplemental References 1.

ACKNOWLEDGMENTS

We thank Candida Nibau and Fiona Corke for their critical reading of the article. We also thank Tomomichi Fujita and Mitsuyasu Hasebe for pCTRN-NPTII2 and pTFH15.3, Mari Obara, Minoru Kubo, and Mitsuyasu Hasebe for pCerulean-NPTII, and Tomoaki Nishiyama and Mitsuyasu Hasebe for pTN186. Microscopy was conducted at the Institute of Transformative Bio-Molecules at Nagoya University and supported by the Japan Advanced Plant Science Research Network. This work was supported by the Japan Society for the Promotion of Science (Grants-in-Aid for Scientific Research 16770039 to Y.H. and 25650075 to Y.S.) and by the European Commission (FP7 Marie Curie Fellowship 275257 to Y.H.).

AUTHOR CONTRIBUTIONS

Y.H. designed the project. Y.H. and Y.S. performed specific experiments and analyzed data with J.H.D. Y.H. and J.H.D. wrote the article. Y.H., Y.S., and J.H.D. revised and edited the article.

Received December 11, 2013; revised February 15, 2014; accepted February 22, 2014; published March 18, 2014.

REFERENCES

Anderhag, P., Hepler, P.K., and Lazzaro, M.D. (2000). Microtubules and microfilaments are both responsible for pollen tube elongation in the conifer *Picea abies* (Norway spruce). Protoplasma **214:** 141–157.

Ashton, N.W., and Cove, D.J. (1977). The isolation and preliminary characterization of auxotrophic and analogue resistant mutants in the moss *Physcomitrella patens*. Mol. Gen. Genet. **154:** 87–95.

Bibikova, T.N., Blancaflor, E.B., and Gilroy, S. (1999). Microtubules regulate tip growth and orientation in root hairs of *Arabidopsis thaliana*. Plant J. **17:** 657–665.

Brown, R.C., and Lemmon, B.E. (2001). The cytoskeleton and spatial control of cytokinesis in the plant life cycle. Protoplasma **215:** 35–49.

Cai, G., and Cresti, M. (2010). Microtubule motors and pollen tube growth—Still an open question. Protoplasma **247:** 131–143.

Chan, J., Calder, G.M., Doonan, J.H., and Lloyd, C.W. (2003). EB1 reveals mobile microtubule nucleation sites in *Arabidopsis*. Nat. Cell Biol. **5:** 967–971.

Doonan, J.H., Cove, D.J., and Lloyd, C.W. (1988). Microtubules and microfilaments in tip growth: Evidence that microtubules impose polarity on protonemal growth in *Physcomitrella patens*. J. Cell Sci. **89:** 533–540.

Fischer, R., Zekert, N., and Takeshita, N. (2008). Polarized growth in fungi—Interplay between the cytoskeleton, positional markers and membrane domains. Mol. Microbiol. **68:** 813–826.

Griesbeck, O., Baird, G.S., Campbell, R.E., Zacharias, D.A., and Tsien, R.Y. (2001). Reducing the environmental sensitivity of yellow fluorescent protein: Mechanism and applications. J. Biol. Chem. **276:** 29188–29194.

Hepler, P.K., and Jackson, W.T. (1968). Microtubules and early stages of cell-plate formation in the endosperm of *Haemanthus katherinae* Baker. J. Cell Biol. **38:** 437–446.

Hiwatashi, Y., Nishiyama, T., Fujita, T., and Hasebe, M. (2001). Establishment of gene-trap and enhancer-trap systems in the moss *Physcomitrella patens*. Plant J. **28:** 105–116.

Hiwatashi, Y., Obara, M., Sato, Y., Fujita, T., Murata, T., and Hasebe, M. (2008). Kinesins are indispensable for interdigitation of phragmoplast microtubules in the moss *Physcomitrella patens*. Plant Cell **20:** 3094–3106.

Ho, C.M., Hotta, T., Guo, F., Roberson, R.W., Lee, Y.R., and Liu, B. (2011). Interaction of antiparallel microtubules in the phragmoplast is mediated by the microtubule-associated protein MAP65-3 in *Arabidopsis*. Plant Cell **23:** 2909–2923.

Honnappa, S., et al. (2009). An EB1-binding motif acts as a microtubule tip localization signal. Cell **138:** 366–376.

Idilli, A.I., Morandini, P., Onelli, E., Rodighiero, S., Caccianiga, M., and Moscatelli, A. (2013). Microtubule depolymerization affects endocytosis and exocytosis in the tip and influences endosome movement in tobacco pollen tubes. Mol. Plant **6:** 1109–1130.

Justus, C.D., Anderhag, P., Goins, J.L., and Lazzaro, M.D. (2004). Microtubules and microfilaments coordinate to direct a fountain streaming pattern in elongating conifer pollen tube tips. Planta **219:** 103–109.

Konzack, S., Rischitor, P.E., Enke, C., and Fischer, R. (2005). The role of the kinesin motor KipA in microtubule organization and polarized growth of *Aspergillus nidulans*. Mol. Biol. Cell **16:** 497–506.

Kubo, M., Imai, A., Nishiyama, T., Ishikawa, M., Sato, Y., Kurata, T., Hiwatashi, Y., Reski, R., and Hasebe, M. (2013). System for stable β-estradiol-inducible gene expression in the moss *Physcomitrella patens*. PLoS ONE **8:** e77356.

Lazzaro, M.D., Marom, E.Y., and Reddy, A.S. (2013). Polarized cell growth, organelle motility, and cytoskeletal organization in conifer pollen tube tips are regulated by KCBP, the calmodulin-binding kinesin. Planta **238:** 587–597.

Lee, Y.R., Giang, H.M., and Liu, B. (2001). A novel plant kinesin-related protein specifically associates with the phragmoplast organelles. Plant Cell **13:** 2427–2439.

Menand, B., Calder, G., and Dolan, L. (2007). Both chloronemal and caulonemal cells expand by tip growth in the moss *Physcomitrella patens*. J. Exp. Bot. **58:** 1843–1849.

Merzlyak, E.M., Goedhart, J., Shcherbo, D., Bulina, M.E., Shcheglov, A.S., Fradkov, A.F., Gaintzeva, A., Lukyanov, K.A., Lukyanov, S., Gadella, T.W., and Chudakov, D.M. (2007). Bright monomeric red fluorescent protein with an extended fluorescence lifetime. Nat. Methods **4:** 555–557.

Murata, T., Sano, T., Sasabe, M., Nonaka, S., Higashiyama, T., Hasezawa, S., Machida, Y., and Hasebe, M. (2013). Mechanism of microtubule array expansion in the cytokinetic phragmoplast. Nat. Commun. **4:** 1967.

Nishiyama, T., Hiwatashi, Y., Sakakibara, I., Kato, M., and Hasebe, M. (2000). Tagged mutagenesis and gene-trap in the moss, *Physcomitrella patens* by shuttle mutagenesis. DNA Res. **7:** 9–17.

Petrásek, J., and Schwarzerová, K. (2009). Actin and microtubule cytoskeleton interactions. Curr. Opin. Plant Biol. **12:** 728–734.

Rizzo, M.A., Springer, G.H., Granada, B., and Piston, D.W. (2004). An improved cyan fluorescent protein variant useful for FRET. Nat. Biotechnol. **22:** 445–449.

Rounds, C.M., and Bezanilla, M. (2013). Growth mechanisms in tip-growing plant cells. Annu. Rev. Plant Biol. **64:** 243–265.

Schindelin, J., et al. (2012). Fiji: An open-source platform for biological-image analysis. Nat. Methods **9:** 676–682.

Schuchardt, I., Assmann, D., Thines, E., Schuberth, C., and Steinberg, G. (2005). Myosin-V, Kinesin-1, and Kinesin-3 cooperate in hyphal growth of the fungus *Ustilago maydis*. Mol. Biol. Cell **16:** 5191–5201.

Shen, Z., Collatos, A.R., Bibeau, J.P., Furt, F., and Vidali, L. (2012). Phylogenetic analysis of the Kinesin superfamily from *Physcomitrella*. Front Plant Sci **3:** 230.

Steinberg, G. (2007a). Hyphal growth: A tale of motors, lipids, and the Spitzenkörper. Eukaryot. Cell **6:** 351–360.

Steinberg, G. (2007b). Preparing the way: Fungal motors in microtubule organization. Trends Microbiol. **15:** 14–21.

Timmers, A.C.J., Vallotton, P., Heym, C., and Menzel, D. (2007). Microtubule dynamics in root hairs of *Medicago truncatula*. Eur. J. Cell Biol. **86:** 69–83.

Vidali, L., and Bezanilla, M. (2012). *Physcomitrella patens*: A model for tip cell growth and differentiation. Curr. Opin. Plant Biol. **15:** 625–631.

Vidali, L., Rounds, C.M., Hepler, P.K., and Bezanilla, M. (2009). Lifeact-mEGFP reveals a dynamic apical F-actin network in tip growing plant cells. PLoS ONE **4:** e5744.

Wang, X., Zhu, L., Liu, B., Wang, C., Jin, L., Zhao, Q., and Yuan, M. (2007). *Arabidopsis* MICROTUBULE-ASSOCIATED PROTEIN18 functions in directional cell growth by destabilizing cortical microtubules. Plant Cell **19:** 877–889.

Yang, G., Gao, P., Zhang, H., Huang, S., and Zheng, Z.L. (2007). A mutation in *MRH2* kinesin enhances the root hair tip growth defect caused by constitutively activated ROP2 small GTPase in *Arabidopsis*. PLoS ONE **2:** e1074.

Zhu, C., and Dixit, R. (2012). Functions of the *Arabidopsis* kinesin superfamily of microtubule-based motor proteins. Protoplasma **249:** 887–899.

Zhu, L., Zhang, Y., Kang, E., Xu, Q., Wang, M., Rui, Y., Liu, B., Yuan, M., and Fu, Y. (2013). MAP18 regulates the direction of pollen tube growth in *Arabidopsis* by modulating F-actin organization. Plant Cell **25:** 851–867.